Self-complementary AAV Virus (scAAV) Safe and Long-term Gene Transfer in the Trabecular Meshwork of Living Rats and Monkeys

LaKisha K. Buie,[1] Carol A. Rasmussen,[2] Eric C. Porterfield,[1] Vinod S. Ramgolam,[3] Vivian W. Choi,[4] Silva Markovic-Plese,[3,5] Richard J. Samulski,[4] Paul L. Kaufman,[2] and Teresa Borrás[1]

Purpose. AAV vectors produce stable transgene expression and elicit low immune response in many tissues. AAVs have been the vectors of choice for gene therapy for the eye, in particular the retina. scAAVs are modified AAVs that bypass the required second-strand DNA synthesis to achieve transcription of the transgene. The goal was to investigate the ability of AAV vectors to induce long-term, safe delivery of transgenes to the trabecular meshwork of living animals.

Methods. Single doses of AAV2.GFP and AAV2.RGD.GFP/Ad5.LacZ were injected intracamerally (IC) into rats (n = 28 eyes). A single dose of scAAV.GFP was IC-injected into rats (n = 72 eyes) and cynomolgus monkeys (n = 3). GFP expression was evaluated by fluorescence, immunohistochemistry, and noninvasive gonioscopy. Intraocular pressure (IOP) was measured with calibrated tonometer (rats) and Goldmann tonometer (monkeys). Differential expression of scAAV-infected human trabecular meshwork cells (HTM) was determined by microarrays. Humoral and cell-mediated immune responses were evaluated by ELISA and peripheral blood proliferation assays.

Results. No GFP transduction was observed on the anterior segment tissues of AAV-injected rats up to 27 days after injection. In contrast, scAAV2 transduced the trabecular meshwork very efficiently, with a fast onset (4 days). Eyes remained clear and no adverse effects were observed. Transgene expression lasted >3.5 months in rats and >2.35 years in monkeys.

Conclusions. The scAAV viral vector provides prolonged and safe transduction in the trabecular meshwork of rats and monkeys. The stable expression and safe properties of this vector could facilitate the development of trabecular meshwork drugs for gene therapy for glaucoma. (*Invest Ophthalmol Vis Sci.* 2010;51:236–248) DOI:10.1167/iovs.09-3847

From the Departments of [1]Ophthalmology, [3]Neurology, and [5]Microbiology and Immunology and the [4]Gene Therapy Center, University of North Carolina School of Medicine, Chapel Hill, North Carolina; and the [2]Department of Ophthalmology and Visual Sciences, University of Wisconsin School of Medicine and Public Health, Madison, Wisconsin.

Supported by National Institutes of Health Grants EY11906 (TB) and EY13126 (TB), KO8 NS045871-01 (SM), HL051818 (RJS), 1R01EY019555-01 (RJS), EY02698 (PLK), P30 EY016665 (UWSMPH) (PLK); The Ocular Physiology Research and Education Foundation (PLK); and the Research to Prevent Blindness (UW and UNC).

Submitted for publication April 10, 2009; revised July 13, 2009; accepted July 14, 2009.

Disclosure: **L.K. Buie**, None; **C.A. Rasmussen**, None; **E.C. Porterfield**, None; **V.S. Ramgolam**, None; **V.W. Choi**, None; **S. Markovic-Plese**, None; **R.J. Samulski**, None; **P.L. Kaufman**, None; **T. Borrás**, None

Corresponding author: Teresa Borrás, Department of Ophthalmology, University of North Carolina School of Medicine, 6109 Neuroscience Research Building CB 7041, 105 Mason Farm Road, Chapel Hill, NC 27599-7041; tborras@med.unc.edu.

The cells of the outflow pathway of the eye are ideal targets for gene transfer for many specific reasons. Their location, morphology, and physiology all seem to be tailored for efficient gene delivery. First, because of the natural flow of aqueous humor, genes delivered into the anterior chamber preferentially reach the trabecular meshwork. Second, once the vectors reach the trabecular meshwork, the physiological flow pattern of the fluid between and around the trabecular meshwork cell layers provides the transfer molecules with a longer contact time and facilitates their entry into the cells. Another advantage is the spongiform loose structure and optically empty spaces of the tissue architecture, which allows direct access of the transfer molecules to most cells. Fluid crossing through the inner wall monolayer of Schlemm's canal (SC) further permits the transfer molecules to directly contact the Schlemm's canal cells. Finally, the anterior chamber is an immune privileged site.[1] Collectively, these properties offer the opportunity to alter gene expression in the trabecular meshwork and investigate the contribution of a given gene-encoded mechanism to the maintenance of aqueous humor outflow resistance. Most important, gene transfer to the trabecular meshwork would facilitate efficient development of more precisely targeted and less toxic drugs for the treatment of glaucoma, a chronic disease that affects more than 70 million people worldwide.[2,3]

Several viral vectors have been used to transfer genes to the trabecular meshwork in living animals. Recombinant ΔE1/E3 adenoviruses transduce the trabecular meshwork tissue very efficiently. Reports of the use of this viral vector have shown functional expression in the trabecular meshwork of all animals studied, from rodents to monkeys.[4–8] Although at high concentrations delivery of adenoviruses can induce an immune response,[7,9] intraocular injections at appropriate concentrations are well tolerated in mice, rats, rabbits, monkeys, and humans.[7,10–14] However, their length of expression is short, with reported durations of 1 to 3 weeks in most animals,[5,7] and in monkeys, repetitive injections were not always well tolerated.[7] These properties would make the use of adenoviruses in glaucoma therapy problematic, given the chronicity of the disease.[7] The transient transgene expression of the adenoviral vectors has been attributed almost equally to the elimination of the cells infected with the virus[15] and to the silencing of their cytomegalovirus (CMV) promoter.[16] Lentiviral vectors, such as the feline immunodeficiency virus (FIV) have been shown to transduce the trabecular meshwork of living cats and monkeys with reported durations thus far up to 2.3 and 1.25 years, respectively.[17,18] However, the lentiviral vector strain derived

from the human immunodeficiency virus type 1 using an elongation factor (EF-1α) promoter, transduced the trabecular meshwork of rats for just 3 weeks.[19]

Because of their stable, long-term expression and their low immunogenicity, adeno-associated viral vectors (AAV) have been the vectors of choice for gene therapy for the retina. AAV vectors are used in most retinal ganglion cell (RGC) survival studies,[20,21] as well as in those involving retinal degeneration models.[22,23] Furthermore, AAV was the vector used in the first case of restoration of visual function in a dog model of Leber amaurosis.[23] This AAV is currently in phase I gene therapy clinical trials showing improved vision and no adverse effects in three young adults with inherited blindness.[24] AAVs are defective parvoviruses that contain a 4.7-kb single-stranded (ss) DNA flanked by inverted terminal repeats.[25,26] They require a helper adenovirus for infection, and their genome encodes the AAV proteins needed for replicating and packaging. On entering the cell, the viral ss DNA is converted into a transcriptionally active double-stranded DNA by host enzymes.[25,26] A recombinant AAV vector replaces the DNA encoding both of its viral proteins by a transgene expression cassette and therefore does not contain any open viral reading frames. This replacement allows transgene insert sizes of approximately 4.5 kb, which is an adequate size to accommodate the coding regions of most of the polymerase II genes. AAV vectors infect and transfer genes to dividing and nondividing cells, and methods have been developed to easily grow them to high titers without the need of the helper adenovirus.[27,28] In a good number of animal models and clinical trials in which AAV transgene expression lasted for a long time (5 years in primates),[29] no immunologic response to the transgene was found.[30] However, certain combinations of AAV transgenes and target tissues have induced an immune response.[31,32] It is currently thought that this occasional response depends on several factors such as the nature of the transgene, the promoter used, the route and site of administration, the vector dose, and host factors.[30,32,33] Altogether, the attractive features offered by AAV vectors have made them among the most widely used in clinical trials.[34]

However, AAV vectors are unable to transduce trabecular meshwork cells.[8,35] Our laboratory has recently shown that the lack of transduction of AAV to these cells was not due to a failure of viral entry but rather to an inability of the host cells to convert the viral ss DNA to double stranded.[36] In the same study, we showed that the trabecular meshwork (cells and organ cultured tissue) could be efficiently transduced by the new generation self-complementary AAV (scAAV),[37,38] which bypasses the required second-strand DNA synthesis to achieve the transcriptionally active AAV genome. The recombinant scAAV DNA contains one mutated and one wild-type terminal repeat flanking the expression cassette. After several AAV replication forks, this feature allows the generation of an ss viral genome carrying both sense and complimentary cDNA of the transgene, separated by the mutated terminal repeat and flanked by wild-type repeats. On entry into the host, both strands pair with each other generating the AAV double-stranded DNA needed for transcription.[39] The scAAV expression cassette's size is reduced from the original 4.5 to 2.2. kb which, although smaller, would still allow expression of most trabecular meshwork candidate genes (cDNA of approximately $\leq$1500 bp).[40,41]

In the present study, we extended our investigations with scAAV from in vitro experiments to living animals. We report that a single intracameral injection of an scAAV viral vector confers stable long-term expression of a reporter gene in the trabecular meshwork of living rats (>3.5 months) and monkeys (>2 years) with an early onset and a safe clinical profile.

Methods

Experimental Animals

All animal procedures were approved by the Institutional Animal Care and Use Committee at the University of North Carolina (UNC) and the University of Wisconsin (UW) and were conducted in accordance with the tenets of the Declaration of Helsinki and the ARVO Statement for the Use of Animals in Ophthalmic and Vision Research. Rat strains were either male Brown Norway (300–400 g) retired breeders or male Wistar (200–300 g) and were purchased from Charles River Laboratories (Wilmington, MA). All animals were housed in standard 12-hour cycle lighting with food and water provided ad libitum. Twenty animals were used for the AAV2 study (all Brown Norway) and 53 animals were used for the scAAV2 study (10 Brown Norway and 43 Wistar). One group of six rats was excluded from the analysis because of technical problems.

Three male and three female cynomolgus macaques (*Macaca fascicularis*), 8 to 17 years of age, weighing 5.8 to 6.8 kg, acquired from Covance (Vienna, VA) and Pfizer Laboratories (New York, NY), were used in the study. All monkeys were housed in standard 12-hour cycle lighting with water provided ad libitum and food, twice daily. A detailed enrichment program was used that included social housing, toys and other objects to manipulate, cage furniture, foraging devices, a small manipulable mirror, fruit, and other nutritive snacks, radio, and TV and movies.

Viral Vectors

Recombinant adeno-associated vectors—AAV2.GFP, AAV2.RGD.GFP, and scAAV2.GFP— contained the enhanced GFP gene driven by human enhanced cytomegalovirus (CMV) promoter. They were all prepared by triple-transfection of 293 cells at the University of North Carolina Virus Vector Core, as previously described.[42,43] The viruses were purified by the use of non-ionic iodixanol gradients followed by heparin-affinity chromatography with HPLC columns. Plasmids for the production of AAV2.GFP were pTRUFR, which encodes the GFP expression cassette packaged between the AAV2 terminal repeats; pXX2, which encodes the rep and cap genes; and pXX6–80, which encodes the adenoviral helper function genes.[42] The rep and cap plasmid for AAV2.RGD.GFP (whose capsid contains an RGD peptide) was pA5884C-RGD.[44] The GFP expression cassette was also cloned into the scAAV2 vector construct, with the mutated end of the inverted terminal repeat (ITR) next to the promoter of the gene expression cassette.[37,38] Vector physical particles were assessed by dot blot.

The Ad5.LacZ adenovirus used in the combination injections was purchased from Qbiogen (Montreal, Quebec, Canada) and contains the β-galactosidase gene under the control of the CMV promoter. The virus was grown and purified in our laboratory as described.[45] Virus particle number was determined by measurement of their optical density at 260 nm using the formula 1 μg DNA (2.2×10^{10} viral particles [VP]). The vector AAV2CBA.GFP[46] was generously provided by Thomas J. McCown (Gene Therapy Center, University of North Carolina).

Intraocular Administration of Recombinant Viral Vectors

Each rat was anesthetized by intraperitoneal injection of 1 mL/kg of a standard rat cocktail consisting of a solution of 5 mL ketamine (100 mg/mL), 2.5 mL xylazine (20 mg/mL), 1 mL acepromazine (10 mg/mL), and 1.5 mL of water. While resting on its side, the rat was placed under a surgical microscope with the head propped up in a holder and eyes directed upward. The corneas were anesthetized with 1 drop of 0.5% proparacaine hydrochloride (Alcaine; Alcon, Fort Worth, TX). For the

intracameral vector delivery, a 30-gauge needle was inserted through the cornea at the limbus with the bevel up to gently reach the center of the anterior chamber (AC). The needle device consisted of the tip of a 30-gauge needle, broken at the middle, connected to one end of intramedic-polyethylene tubing (PE-10; Clay Adams, Parsippany, NJ). The remaining half of the needle, plus the hub, was attached at the other end of the tubing and then connected to a dispenser (Gilmont Micrometer; Barnant, Barrington, IL). The tubing was partially filled with a colored glycerol driving solution to allow aspiration of 3 to 5 μL of the viral sample. Inside the tubing, the driving solution was kept separated by 3 to 4 cm from the sample at all times. When the needle was inside the AC, the sample was delivered by the assistant over 30 seconds and fluid entry monitored by direct visualization through the operating microscope. The needle was left in place for 1 to 2 minutes and withdrawn gradually to minimize leaking. Topical antibiotic ointment (neomycin 3.5 mg/g, polymyxin B 10,000 U/g, and bacitracin 400 U/g; Akorn, Lake Forest, IL) was placed on the eyes, and the animals were returned to their cages, resting on absorbent paper for recovery.

The rats' eyes were enucleated immediately after euthanatization and immersed in fresh 4% paraformaldehyde in PBS for 30 minutes. The eyes were then opened at the equator, the lens removed, and wedge shape specimens containing the anterior chamber angle region with the trabecular meshwork fixed for an additional hour. Specimens were then consecutively washed in 10% sucrose (6 hours) and 30% sucrose (overnight) and frozen in OCT (Tissue-Tek; Sakura Finetek, Torrance, CA) in liquid nitrogen. Meridional 10-μm sections were mounted on microscope slides (Superfrost/Premium; Thermo Fisher, Waltham, MA, with Fluoromont G; Southern Biotechnology Associates, Birmingham, AL) and GFP was visualized with a fluorescence microscope (model IX71; Olympus, Tokyo, Japan). Images were captured with a digital camera (DP70; Olympus) and accompanying software. Digital images were arranged with image-analysis software (Photoshop CS; Adobe Photoshop, Mountain View, CA).

Specimens from monkey 3 and perfused monkey anterior segments were shipped to UNC in a container with a small amount of saline, packed in ice and processed, fixed, and analyzed as just described. For immunohistochemistry, 10-μm frozen sections were blocked with 10% goat serum in PBS for 30 minutes followed by overnight incubation with Alexa Fluor 594-conjugated anti-GFP monoclonal antibody (Invitrogen, Carlsbad, CA), 1:1000 diluted in 10% goat serum, and 0.3% Tween in PBS. The washing buffer was PBS (three times, 10 minutes each). The sections were then mounted and analyzed as described for fluorescence histochemistry.

For vector administration, the monkeys were anesthetized (ketamine HCl, 10 mg/kg, supplemented with 5 mg/kg, and medetomidine 15–75 μg/kg), and a 30-μL bolus, 3×10^{10} VP, of scAAV2.GFP vector preparation was injected transcorneally, in 15-μL increments, into the anterior chamber. Vector solutions were injected with a 30-gauge needle connected to a micrometer syringe with polyethylene (PE 10) tubing. Under microscopic visualization, the needle was threaded through the cornea for several millimeters, and the tip angled into the anterior chamber. The needle was left in place for 2 minutes after vector injection to allow for tubing hysteresis to subside. No fluid leakage was observed during needle withdrawal.

Gonioscopy and Goniophotography

The monkeys were regularly examined with a slit lamp biomicroscope for corneal and lenticular clarity and for evidence of anterior chamber cells and flare. GFP expression was monitored serially and noninvasively as previously described.[7] Briefly, a drop of 0.5% proparacaine hydrochloride was instilled, and a Swan-Jacob gonioscopy lens was placed on the corneal surface of ketamine-anesthetized (10 mg/kg, intramuscular initial, supplemented with 5 mg/kg, as needed), supine monkeys, to view the structures in and adjacent to the iridocorneal angle. A retinal camera (50EX; Topcon, Tokyo, Japan), fitted with a digital SLR camera body (D1X; Nikon) and the standard clinical fluorescein exciter and barrier filters, was used to photograph the angle. A customized microscope (Nikon Instruments, Inc., Melville, NY) with a 12-bit, monochromatic, cooled-CCD camera (Retiga 2000RV; Q-Imaging Burnaby, BC, Canada) and a specific GFP filter set was also used to collect images of the angle at several time points. Another imaging configuration used to collect color images of the angle combined the digital camera with a 175-W xenon nova light source and a 3-mm $\times$ 6-cm 0° tele-otoscope probe (Hopkins II; Karl Storz Endoscopy-America, Inc., Culver City, CA). A drop of 0.5% proparacaine hydrochloride was placed on the cornea, and 2.5% hydroxypropyl methylcellulose was used as an interface between the tip of the probe and the cornea.

Measurement of Rat and Monkey Intraocular Pressure

Intraocular pressures (IOP) were recorded in sedated rats once or twice a week. At the beginning of the study, IOPs were recorded with a calibrated handheld tonometer (Tonopen XL; Mentor, Norwell, MA) and midway through the study, IOPs were measured by the use of the rebound tonometer.[47] The tonometer was calibrated by inserting a needle into the anterior chamber of anesthetized rats and connecting it to a column of water. The rebound tonometer instrument used was one of the prototypes developed at Mount Sinai School of Medicine (New York) and was generously provided to us by Thomas Mittag and John Danias.[47,48] The rats were lightly anesthetized with the described intraperitoneal ketamine/xylazine/acepromazine cocktail at half dose and with an eye drop of 0.5% proparacaine. To take IOP measurements, the rats were positioned with the visual axis horizontal to the probes. For the tonometer, IOPs were obtained as the average of 10 consecutive measurements for each eye. For the rebound tonometer, the probe was held at a distance between 2 and 5 mm and five consecutive readings (arbitrary units that correlate to IOP) were obtained by pressing the foot pedal connected to the probe power supply. Only mean values with a standard deviation (expressed as percentage of the mean) less than 5% were accepted. The rebound tonometer was calibrated on rats at the same ages as those used in the experiments (before and 3.5 months after injection) by ex vivo cannulation and manometric readings as described.[47] IOP-correlated values were obtained by creating a logarithmic calibration curve with the tonometer and manometric values and obtaining the a and b constant values in the calibration curve formula [$Y = a\text{Ln}(X) - b$], where X is the correlated IOP and Y is the tonometer's measurement. The correlated IOP (X) = [exponent(tonometer value + b)/a)]. The calibration curves had correlation coefficients of 0.98 and 0.96, respectively.

Monkey IOP was measured with a minified Goldmann tonometer in ketamine anesthetized (10 mg/kg, intramuscular initial, supplemented with 5 mg/kg, as needed), supine monkeys.[49] Nondairy creamer was used as a tear film interface instead of fluorescein (which could potentially confound the subsequent examinations) to determine presence and location of the GFP marker. Measurements were taken every 3 to 4 days for the first 2 weeks, weekly for 4 to 6 weeks, then every 2 to 4 weeks. IOP measurements were usually performed before and on the same day as slit lamp biomicroscopy and goniophotography, to minimize exposure to anesthesia.

Outflow Facility Cells

To generate primary human trabecular meshwork (HTM) cells, the trabecular meshwork was dissected from a residual cornea rim after surgical corneal transplantation at the UNC eye clinic. Specimens were cut in small pieces, carefully attached to the bottom of a 2% gelatin-coated 35-mm dish, and covered with a drop of medium (improved minimal essential medium [IMEM], 20% fetal bovine serum [FBS], 50 μg/mL gentamicin) and a coverslip. Dishes were incubated in a humidified 6% CO_2 atmosphere, medium was changed every other day, and the cells were allowed to grow from the explant for a period of 4 weeks. Once confluent, the cells were passed to a T-25 flask and labeled as passage 1. Subsequently, cells were passed 1:4 to confluence and maintained in the same medium with 10% FBS. All cells were used at passages 4 to 6. These outflow pathway cultures include the cells

from the three distinct regions of the trabecular meshwork plus cells lining the SC. Because most of the cells in these cultures come from the trabecular meshwork, they are commonly referred to as trabecular meshwork cells. The cells used in this study were from a 29-year-old donor (HTM-63).

RNA Extraction and Hybridization to Gene Microarrays

The primary human trabecular cell line HTM-63 was grown to 80% confluence and infected with scAAV2.GFP (~1400 VP/cell). Total RNA from 10-cm plates infected and uninfected dishes was extracted 5 days after infection. Cellular pellets were resuspended in guanidine thiocyanate buffer (RLT; Qiagen, Chatsworth, CA) and loaded onto a column (QIAshredder; Qiagen), and the extraction was continued (RNeasy Mini kit with on-column RNase-free DNase digestion; Qiagen), according to the manufacturer's directions. Total RNA recoveries averaged 30 μg per plate.

The RNAs were prepared for hybridization to human genome microarrays (U133A GeneChips, $n = 2$; Affymetrix, Santa Clara CA) at the UNC Functional Genomics Core Facility. Seven micrograms of total RNA was used to synthesize cDNA. A custom cDNA kit from Life Technologies (Gaithersburg, MD) was used with a T7-$(dT)_{24}$ primer for this reaction. Biotinylated cRNA was then generated from the cDNA reaction (BioArray High Yield RNA Transcript Kit; Enzo Life Sciences, Farmingdale, NY). The cRNA was then fragmented in fragmentation buffer (5× fragmentation buffer: 200 mM Tris-acetate [pH 8.1], 500 mM KOAc, and 150 mM MgOAc) at 94°C for 35 minutes before the chip hybridization. Fifteen micrograms of fragmented cRNA was then added to a hybridization cocktail (0.05 μg/μL fragmented cRNA, 50 pM control oligonucleotide B2, *BioB*, *BioC*, *BioD*, and *cre* hybridization controls, 0.1 mg/mL herring sperm DNA, 0.5 mg/mL acetylated BSA, 100 mM MES, 1 M $[Na^+]$, 20 mM EDTA, and 0.01% Tween 20). Ten micrograms of cRNA was used for hybridization. Arrays were hybridized for 16 hours at 45°C (GeneChip Hybridization Oven 640; Affymetrix). The arrays were washed and stained with R-phycoerythrin streptavidin (GeneChip Fluidics Station 400; Affymetrix). After this, the arrays were scanned (GeneArray Scanner; Hewlett Packard). Microarray software (xGeneChip Microarray Suite 5.0; Affymetrix) was used for washing, scanning, and basic analysis. Sample quality was assessed by examination of 3′ to 5′ intensity ratios of certain genes.

A different primary cell line HTM-109 was infected with a lower number of scAAV2.GFP VP (~140 VP/cell) and RNA extracted at 5 days after infection. RNAs were hybridized to a second set of microarrays ($n = 2$; Human Genome U133A GeneChip; Affymetrix), treated, and analyzed as just described.

Reverse Transcription and Real-Time PCR

Reverse transcription (RT) reactions were conducted with 1 μg of HTM cells spectrophotometrically measured, total RNA in a 25-μL total volume of proprietary RT buffer containing random primers, dNTPs, and 62.5 U of enzyme with RNase inhibitor (Multiscribe MuLV RT; High Capacity cDNA kit; ABI), according to the manufacturer's recommendations (25°C for 10 minutes, 37°C for 2 hours).

Fluorescently labeled probes/primers sets were used for selected genes (*Taq*Man Gene Expression collection; ABI). The Matrix Gla probe (MGP) corresponded to sequences from exons 1 and 2 (Hs00179899_m1), the osteoglycin (OGN) probed corresponded to sequences from exons 3 and 4 (Hs00247901_m1), the secretogranin (SCG2) probe corresponded to sequences from exons 1 and 2 (Hs00185761_m1), and the 18S RNA probe corresponded to sequences surrounding position nucleotide 609 (Hs99999901_s1). Reactions were performed in 20-μL aliquots with master mix (*Taq*Man Universal PCR; no AmpErase UNG; ABI), run on a real-time PCR system (model 7500; ABI) and analyzed (7500 System SDS software; ABI). Relative quantification (RQ) values between treated and untreated samples were calculated by the formula $2^{-\Delta\Delta CT}$, where C_T is the cycle at threshold (automatic measurement), ΔC_T is C_T of the assayed gene minus C_T of the endogenous control (18S), and $\Delta\Delta C_T$ is the ΔC_T of the normalized assayed gene in the treated sample minus the ΔC_T of the same gene in the untreated sample (calibrator). Because of the high abundance of the 18S rRNA used as endogenous control and to get a linear amplification, RT reactions from control and experimental samples were diluted 10^4 times before their hybridization of the 18S probe (*Taq*Man; ABI). Relative quantifications ≥ 1 corresponded to increased changes (*x*-fold). Relative quantifications <1 corresponded to a fraction of the gene expression and were converted to decreased changes by the formula $-1/2^{-\Delta\Delta CT}$. That is, an RQ of 4 corresponded to an increased expression of fourfold (+4), whereas an RQ of 0.25 corresponds to a reduction in expression of fourfold (−4).

Microarray Expression Analyses

Raw data CEL files from Affymetrix were imported into expression analysis software (GeneSpring GX, ver. 7.3.1; Agilent Technologies, Santa Clara, CA). For analysis of expression changes between the infected and uninfected samples, files were preprocessed with the Robust Multichip Average (RMA) and normalized using the Data-Transformation and 50th Percentile normalization algorithms. The data-transformation normalization sets any measurements less than a specified cutoff value (default 0.01) to the cutoff value; it ensures that no negative values are loaded. The 50th percentile normalization step divides the expression values of each chip by the median of all expression values; it ensures that the expression values for each chip can be compared. The normalized data were subsequently filtered on expression level with a minimum signal value of 50 to eliminate genes expressed at lower levels in at least one of two conditions. To identify the top changers in expression, we subsequently filtered data on change, and genes that exhibited at least a twofold increase or decrease in the scAAV2.GFP-infected cells were selected. Gene lists, gene symbols, heat maps, and overlapping Venn diagrams were obtained by the use of the expression analysis software. Likewise gene ontologies (GOs) were obtained from the biological processes lists (GO SLIMS; Affymetrix) available in the software, which contain subsets of the terms in the whole GO.

Immune Response

Enzyme-Linked Immunosorbent Assay. Sera were obtained by tail vein puncture (rats) and from the femoral vein (monkeys) and stored at −80°C. The samples were analyzed for antibodies to viral capsid proteins and the transgenic protein GFP. High-protein binding ELISA plates (Nunc, Rochester, NY) were coated overnight at 4°C with 10^9 viral particles (VP)/well and 0.25–0.50-μg/well GFP in 100 μL 0.1 M sodium carbonate buffer (pH 9.6). The wells were then washed with PBS containing 0.1% Tween, and blocked with 10% FBS-01% Tween in PBS for 30 minutes at 37°C. After additional washes, the samples were incubated with serum dilutions for 2 hours at 37°C. PBS was used as a negative control. A rabbit anti-AAV2 capsid protein (1:100; U.S. Biologicals, Swampscott, MA) and a mouse monoclonal anti-GFP (1:100; Chemicon, Billerica, MA) served as positive controls. The wells were then washed and incubated with 1:1000 diluted horseradish peroxidase–conjugated goat anti-rabbit (controls; Pierce Thermo Scientific, Rockford, IL) and goat anti-rat or goat anti-monkey (Pierce Thermo Scientific) for 1 hour in the presence of 3% goat serum. The wells were washed again, and the color developed (ABTS Peroxidase Substrate; KPL, Gaithersburg, MD). The plates were read at an optical density of 405 nm in a microplate reader (FLUOstar Optima; BMG LabTechnologies, Durham, NC). Samples were run in duplicate or triplicate and the results expressed as the mean ± SEM. Comparisons between the two groups were analyzed by the Student's *t*-test.

Proliferation Assay. Peripheral blood mononuclear cell (PBMC) proliferation assays were performed to detect antigen-specific proliferative responses against the GFP antigen. PBMC were separated from heparinized venous blood 22 hours after venipuncture by using single-density gradient (Ficoll; GE Healthcare, Piscataway, NJ).[50] Briefly, 5 mL of blood was mixed with 3 mL of PBS and carefully laid

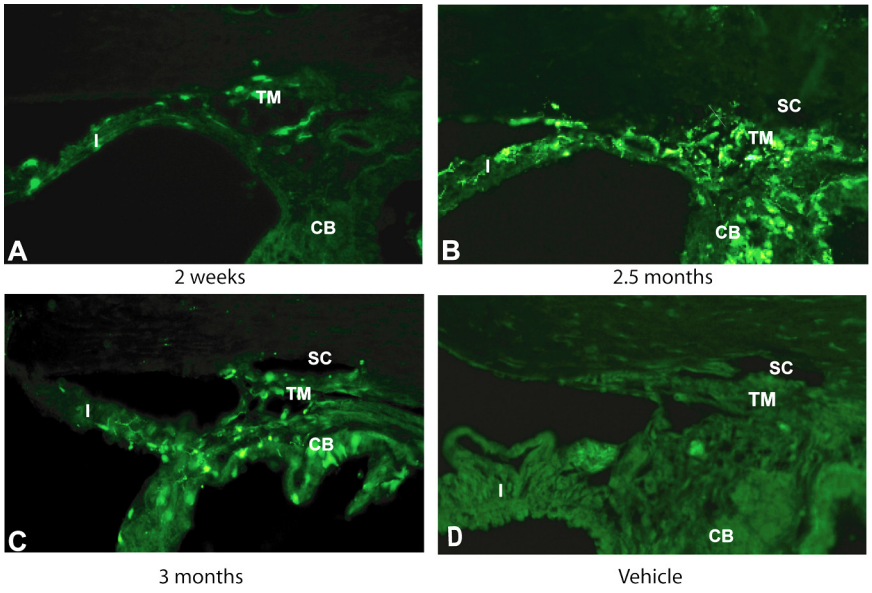

FIGURE 1. Transduction of scAAV2.GFP in the anterior segments of IC-injected rats. Representative frozen meridional sections, 10-μm thick, from rats' anterior segments at various time points. (**A**) scAAV2 transduction of the trabecular meshwork (TM) and iris (I) at 2 weeks after injection. (**B**, **C**) scAAV2 transduction of a variety of tissues including the TM, iris, ciliary body (CB), and corneal endothelium at 2.5 and 3 months after injection. (**D**) Contralateral eyes were injected with vehicle which served as a control. scAAV2.GFP transduced the TM of living rats efficiently. GFP expression lasted for at least 3 months (last point tried). SC, Schlemm's canal. Original magnification, ×200.

on top of 6 mL of gradient in a 15-mL tube. Red blood cells were pelleted by centrifugation at 1500*g* for 30 minutes, and the PMBCs were carefully removed from the gradient interface. The PMBCs were washed twice with PBS and resuspended in 10 mL of RPMI 1640 complete medium supplemented with 10% fetal calf serum, 2 mM glutamine, and 100 U/mL of penicillin G and streptomycin (Invitrogen). Cells (1×10^5) in 200 μL/well were seeded in a 96-well plate and stimulated with 10 μg/well of recombinant GFP (Clontech, Mountain View, CA). Cells cultured in the absence of GFP were used as a negative control. Phorbol 12-myristate 13-acetate (PMA) and ionomycin at 10 and 250 ng/mL, respectively (Sigma-Aldrich, St. Louis, MO) were used as the positive control. Samples were assayed in triplicate. On day 5, the plates were pulsed with 1 μCi/well of [^{3}H]-thymidine (25 Ci/mmol; Amersham Biosciences, Pittsburgh, PA), and cells were harvested after 16 hours. Proliferation ([^{3}H]-thymidine uptake) was assessed by filtration on an automatic cell harvester (ThermoTec, Hutto, TX) and by reading the incorporated radioactivity (filter) on a scintillation plate reader (Wallac MicroBeta Trilux; PerkinElmer, Waltham, MA). The stimulation index (SI) was calculated by dividing the mean counts per minute of [^{3}H]-thymidine incorporated in the GFP-stimulated cells by counts per minute in an unstimulated cell. GFP-specific proliferative response was defined by a SI > 2.

RESULTS

scAAV Overrides Lack of Transduction in the Trabecular Meshwork of Living Rats

In vitro, enhancement of AAV transduction has been shown to occur by co-infecting cultured cells with AAV and wild-type adenoviruses, or AAV with adenovirus capsids alone.[51] Our laboratory also demonstrated that AAV transduction of primary HTM cells is greatly enhanced by co-infecting AAV2 with all recombinant adenoviruses tried.[36] However, Brown Norway and Wistar rats injected intracamerally (IC) with 2×10^{10} to 3×10^{11} VP of AAV2.GFP or AAV2.GFP/Ad5.LacZ combination (40:1) or AAV2.RGD.GFP/Ad5.LacZ showed no GFP transduction on any of the anterior segment tissues at time points from 1 week to 27 days after injection ($n = 28$ eyes). One of the eyes injected with the enhancement combination[36] showed a few green cells in the iris and TM. The same number of particles of an AAV2CBA.GFP injected intravitreally ($n = 4$ eyes) showed intense transduction of the retinal ganglion cells and optic nerve at 2 weeks (not shown).

Because of our previous results showing scAAV2.GFP transduction in HTM cells and perfused human organ cultures,[36] we tested the efficiency of this vector in living animals. Brown Norway and Wistar rat eyes injected IC with 3 to 6×10^9 VP scAAV2.GFP showed positive fluorescence in most tissues of the anterior chamber and in particular, the trabecular meshwork ($n = 72$ eyes; Fig. 1). Fluorescence appeared as soon as 4 to 9 days after injection in the iris ($n = 15$, 14 positive), and showed strong positive trabecular meshwork fluorescence at 2 ($n = 4$), 5 ($n = 15$, 10 positive), and 7 to 9 ($n = 19$, 18 positive) weeks and at 2.5 ($n = 6$, 5 positive) and 3 to 3.5 months ($n = 13$, 5 positive), the last time point. Expression of the GFP driven by the CMV promoter in this viral serotype was directed to the iris, corneal endothelium, ciliary body, ciliary muscle, and especially the layers of the trabecular meshwork including the inner wall of Schlemm's canal. Stationary cultures of the anterior segment showed strong transduction in the trabecular meshwork at 72 hours after infection. No GFP-positive cells were found in the internal layers of the cornea.

scAAV Induction of Long-Term Transduction of the Anterior Segment of the Living Monkey Eye

To test whether scAAV transduction of the trabecular meshwork would occur in a large animal model with an outflow pathway more similar to that of humans, we injected a single dose of 3×10^{10} VP of scAAV2.GFP into the eyes (monkey 1, OS; monkey 2, OD) of two cynomolgus monkeys. The contralateral eye was injected with PBS. A bright green fluorescence was observed as early as 5 days after injection. The fluorescence was strongest in the area of the anterior ciliary muscle and uveal meshwork. By gonioscopy, no difference was observed on the intensity or distribution of the fluorescence between the two monkeys, and thus it appears that both monkeys had the same efficiency of transduction. In monkey 2, same intensity fluorescence continued to be seen and recorded photographically at approximately monthly intervals up to 2.3 years after injection (Fig. 2). Fluorescence was still observed when the manuscript was submitted, and the viral-injected eye remained clear at all times. In monkey 1, fluorescence faded at 70 days after injection after development of an anterior chamber inflammation at 48 days. Although the inflammation was resolved satisfactorily after sub-Tenon steroid injection, no GFP expression was recovered (immune response assessment de-

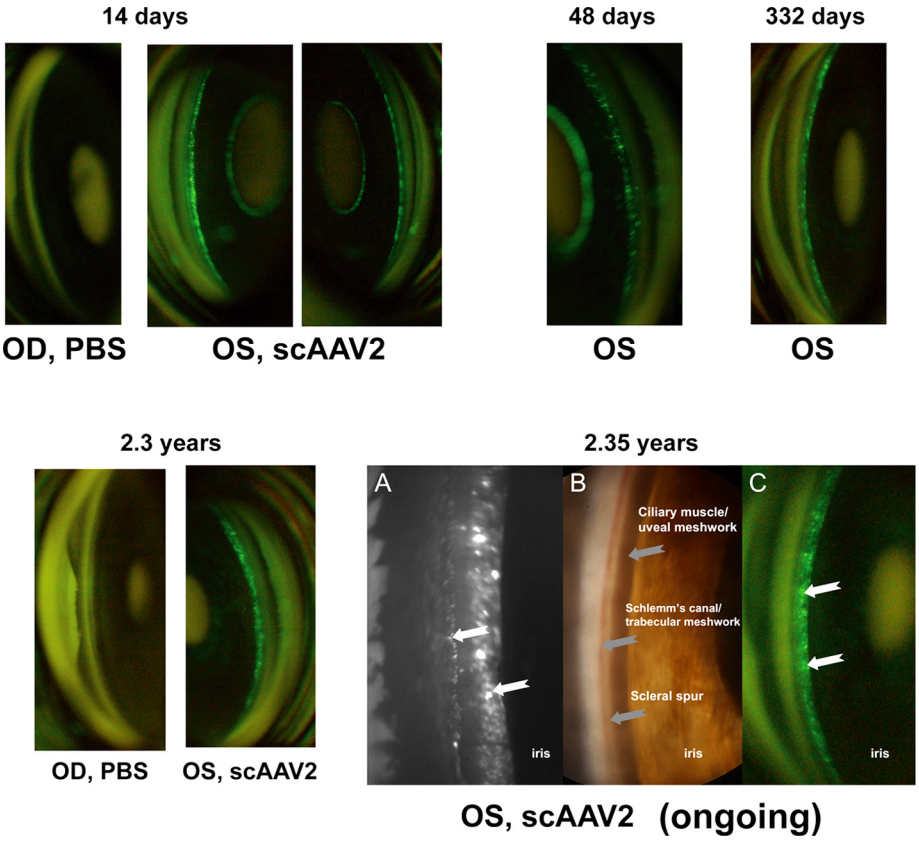

FIGURE 2. scAAV2.GFP vector expression in the anterior segment of monkey 2. Stable, long-term expression, monitored serially and noninvasively with goniophotography, was evident in the tissues of the outflow pathways of the scAAV.GFP-injected eye. Images were taken with a fundus camera on the indicated postinjection days. *Bottom right*: anterior chamber angle, OS, shows persistent GFP expression (**A**, **C** *white arrows*) at 2.35 years. (**A**) Image obtained by custom microscope. (**B**) Image obtained with a Storz endoscope used externally with 2.5% hydroxypropyl methylcellulose as an interface. (**C**) Fundus camera image.

scribed later). In both positive monkeys, evaluation by gonioscopy revealed that fluorescence was brightest in the anterior ciliary muscle, iris processes, and uveal meshwork.

To further assess whether all cell layers of the trabecular meshwork in monkeys were transduced by scAAV2.GFP, we performed two additional experiments. In the first one, a third living monkey was injected at the same dose and killed at 19 days after injection. Anterior segments quadrants were then processed for immunohistochemistry. In the second experiment, monkey anterior segment organ cultures[52] were injected with 2 to 4×10^{10} VP, perfused for 7 to 8 days, and similarly evaluated. Cryosections from both experiments analyzed by both direct fluorescence and GFP antibody showed positive transduction to the trabecular meshwork (Figs. 3A, 3B). As had been observed by in vivo gonioscopy, the sections from the living monkey showed that this scAAV serotype transduced the anterior ciliary muscle with high efficiency (Fig. 3A). In the perfused organ cultures, the trabecular meshwork was also effectively transduced (Fig. 3B).

Histochemical analyses of all other anterior segment tissues from the monkey killed at 19 days showed that the scAAV2 virus had a high tropism for the cells of the posterior face of the iris (Fig. 4). Wholemount as well as histologic sections of the iris showed bright green fluorescent cells almost exclusively on the posterior face. As observed in the living animal by gonioscopy and in cryosections at the end of the experiment, the corneal endothelium appeared highly fluorescently labeled (Fig. 4).

Clinical Signs in Living Rats and Monkeys Injected with scAAV2

Table 1 summarizes the clinical observations. Rat eyes injected with the scAAV2 showed neither opacity nor signs of inflammation at any time during the duration of the experiment and were undistinguishable from the vehicle-injected eye. The viral injected eye of monkey 1 was clear until 48 days after injection, when it developed an anterior segment inflammation that subsequently eliminated the transduced cells (described later). Monkey 2's virus-injected eye, in which expression is still being observed by gonioscopy, showed a clear cornea and no signs of inflammation. Monkey 3 showed trace cells in the anterior chamber at day 6, which cleared by day 14; its corneas remained clear. All the monkeys' eyes were clear at the end of the experiment.

Effect of scAAV Transduction on the IOP of Living Rats and Monkeys

IOPs (mean ± SE) shown in this section and in Figure 5 were obtained with a rebound tonometer[48] and were derived by creating a logarithmic calibration curve with the tonometer and manometric values. Figure 5A shows the results of two rat experiments ($n = 8$ each). Experiment 1 was conducted over 92 ($n = 6$) and 62 ($n = 2$) days, and experiment 2 over 75 days ($n = 8$). Figure 5A shows the absolute IOPs for the vehicle and scAAV injected eyes over time in each animal group. In experiment 1, the IOP averages for the vehicle injected eye were 9.2 ± 0.27 mm Hg at baseline and 11.5 ± 0.14 mm Hg at 92 days after injection, whereas those of the scAAV2-injected eye were 9.2 ± 0.25 mm Hg at baseline and 11.6 ± 0.27 mm Hg at 92 days. In experiment 2, the IOP averages for the vehicle-injected eye were 10.4 ± 0.39 mm Hg at baseline and 11.5 ± 0.21 mm Hg at 75 days after injection, whereas those of the scAAV2-injected eye were 10.4 ± 0.27 mm Hg at baseline and 11.7 ± 0.18 mm Hg at 75 days. The peak IOP (defined as the highest IOP obtained for each eye at any time during the study period) averaged 11.3 ± 0.2 mm Hg for the vehicle-injected (control) eyes and 11.4 ± 0.3 mm Hg for the scAAV2.GFP-

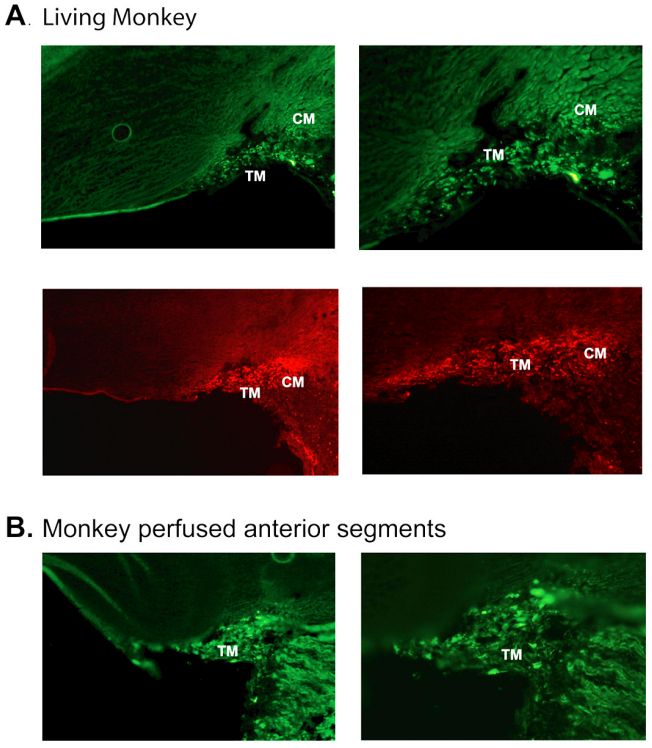

FIGURE 3. Histologic assessment of scAAV2.GFP transduction of monkey trabecular meshwork. (**A**) GFP expression examined by direct fluorescence (*top*) and immunohistochemistry (*bottom*) on OCT-embedded, frozen sections from monkey 3 at 19 days after injection. (**B**) GFP expression examined by direct fluorescence on frozen sections from monkey anterior segment organ cultures perfused with 2 to 4 × 1010 VP of scAAV2.GFP for 7 days. scAAV2.GFP transduced all cell layers of the monkey trabecular meshwork as well as the anterior ciliary muscle. TM, trabecular meshwork; CM, ciliary muscle. Original magnification: (*left*) ×200; (*right*), ×400.

injected (treated) eyes in experiment 1 and 11.6 ± 0.2 and 11.7 ± 0.2 mm Hg, respectively, for experiment 2 (Fig. 5B).

At the end of the experiment, for experiment 1 the ΔIOPs in each group minus their own baseline were 2.4 ± 0.41 mm Hg for the control group and 2.13 ± 0.41 mm Hg for the treated ones. The ΔIOP between the treated and control groups was −0.1 ± 0.38 mm Hg for experiment 1 ($P = 0.89$) and 0.3 ± 0.55 mm Hg for experiment 2 ($P = 0.58$). The peak ΔIOP in experiment 1 was −0.37 ± 0.33 mm Hg at 27 days after injection, whereas in experiment 2, it was 0.3 ± 0.55 mm Hg at 75 days (last day of this experiment). There was no significant difference between the control and treated eyes, showing that the scAAV2 vector carrying a reporter gene is not deleterious for the eye pressures of the rat.

The longitudinal IOP (defined as the mean IOP during the duration of the experiment) was relatively consistent between control and treated groups with values of 10.42 ± 0.17 mm Hg (control) and 10.34 ± 0.20 mm Hg (treated) in experiment 1 and 11.0 ± 0.19 mm Hg (control) and 11.0 ± 0.17 mm Hg (treated) in experiment 2.

The mean integral IOP (defined as the cumulative IOP each animal received during the experiment) of all animals in the experiment 1 group was 978.1 ± 12.5 mm Hg-days for the controls and 977.9 ± 13.0 mm Hg-days for the treated eyes and 824.8 ± 14.1 mm Hg-days for the controls and 827.0 ± 13.1 mm Hg-days for the treated eyes in the experiment 2 group (Figs. 5B, 5C). The integral difference (defined as the cumulative IOP exposure of the treated minus the control) was not significant, with values of 4.9 and 2.2 mm Hg-days for experiments 1 and 2, respectively.

The IOP in monkey 2 averaged 12.7 ± 0.55 mm Hg OS (vehicle-injected) and 13.0 ± 0.67 mm Hg OD (virus-injected) over a span of 208 days after injection. In monkey 1, IOPs were 15.7 ± 0.58 mm Hg OD (vehicle-injected) and 15.9 ± 0.48 mm Hg OS (virus-injected) over a span of 781 days after injection.

Effect of scAAV2.GFP on the Transcriptome of Primary Human Trabecular Meshwork Cells

To gain a first insight on the overall changes induced by scAAV2.GFP viral infection on trabecular meshwork gene expression, we infected primary HTM cells with 1×10^{10} VP (~1400 VP/cell) and used microarray chips to compare their RNA with that of the uninfected control.

Using the algorithms of the microarray software (Microarray Suite 5; Affymetrix) to determine present or absent genes in the chips, we found that overall, the percentage of genes assigned as present was slightly lower in the scAAV2-infected cells (39.9%; 8908/22,283) than in the untreated cells (45.5%; 10,137/22,283). The percentage of absent genes was slightly higher in scAAV2-infected cells, (57.8%; 12,285/22,283) than in untreated cells (52.4%; 11,684/22,283). In addition, the subset of genes that were turned on (absent to present) or turned off (present to absent) by infection of the HTM cells with scAAV2.GFP was very small, amounting to 110 annotated nonredundant genes which were turned on (0.49%) and 41 genes that were turned off (0.18%).

Comparison of expression chips of scAAV2-infected versus untreated cells revealed that the infected cultures had 112 annotated nonredundant genes (0.5%) whose expression was altered more than twofold. Of this, only 10 genes were upregulated while the remaining 102 were downregulated (see Supplementary Table S1, [INSERT URL]). An overall heat-map of the genes altered twofold is shown in Figure 6A, which provides a visual image of the majority of downregulated genes. Heat maps based on nonredundant gene lists from the GO biological processes oxidative stress, immune response, and

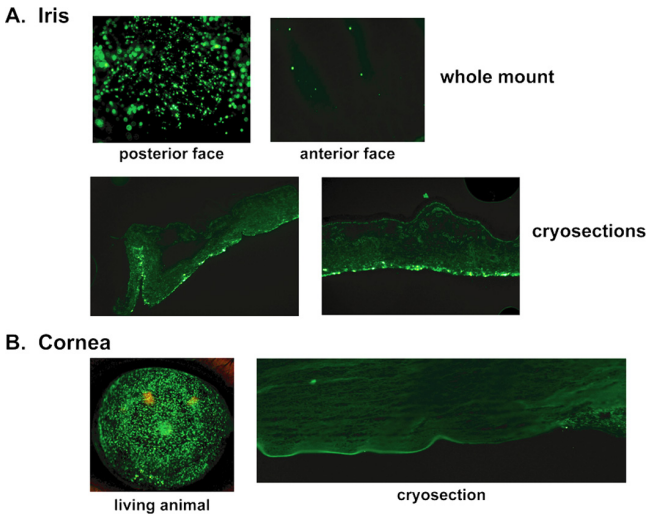

FIGURE 4. scAAV2.GFP transduction of other anterior segment tissues in an IC-injected living monkey. Direct fluorescence of wholemounts and cryosections of the iris (**A**), and goniophotography and cryosection of the cornea (**B**) tissues of monkey 3 at 19 days after injection. Intense GFP transduction was observed in the posterior face of the iris as opposed to the anterior face which had little to no GFP. Strong GFP expression was also observed in the corneal endothelium, especially when assessed by goniophotography in the living animal. Original magnification, ×200.

TABLE 1. Summary of Clinical Signs after scAAV2 Injections

Treatment	Eyes (*n*)	Clarity 1 wk Postinjection	Duration of Expression	Clarity at End of Experiment	Inflammatory Signs during Experiment
Rats					
scAAV2.GFP	68	Clear	98 d	Clear	None
Vehicle	28	Clear	98 d	Clear	None
Monkeys					
scAAV2.GFP					
1	1	Clear	70 d	Clear	AC Inflammation at 48 d
2	1	Clear	2.3y*	Clear	None
3	2	Clear	19 d	Clear	Trace cells at 6 d
Vehicle	2	Clear	2.3y*	Clear	None

Clarity and inflammation in monkeys were assessed biomicroscopically.
* Ongoing expression.

extracellular matrix showed minimal, if any change of expression in the infected cells (Figs. 6B–D).

Because of our interest in specifically determining the effect of scAAV2.GFP on genes that regulate the immune system, we performed Venn maps that identified the number of overlapping genes. A Venn map between the list of genes altered twofold by infection of cells with scAAV2 and the immune response list yielded five genes, all but one of them downregulated in the scAAV2-infected cells (Figs. 7A, 7B). There were no overlapping genes between the twofold list and either the oxidative response or ECM lists (not shown).

Examining the twofold list (Supplementary Table S1, http://www.iovs.org/cgi/content/full/51/1/236/DC1) for the presence of genes relevant to trabecular meshwork function and/or that are part of the trabecular meshwork molecular signature list (Ref. 41 and our unpublished data, 2004–2008) we found six genes, all downregulated in the scAAV2-infected cells. These were secreted frizzled-related protein 1 (*SFRP1*, FC

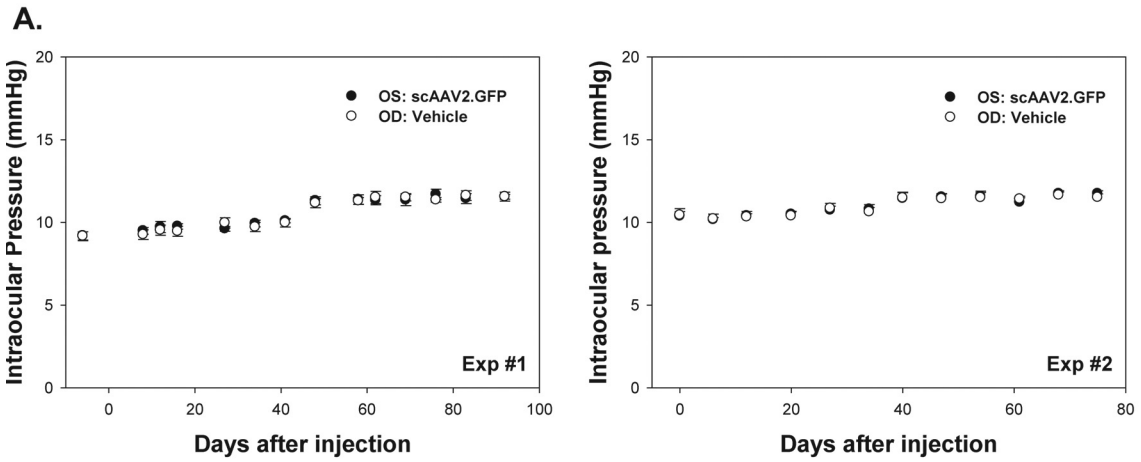

B.

Exp. No.	Treatment	Duration (days)	Integral IOP (mmHg-days)	Integral IOP Difference (mmHg-days)	Peak IOP (mmHg)	Peak IOP Difference (mmHg)
			Mean ± SE		Mean ± SE	
1	scAAV2.GFP	58 (n=8)	585.5 ± 6.5	4.9	11.4 ± 0.3	0.29 ± 0.4
	Vehicle	58 (n=8)	580.5 ± 11.8		11.3 ± 0.2	
	scAAV2.GFP	92 (n=6)	977.9 ± 13.0	-0.13	11.7 ± 0.3	0.23 ± 0.5
	Vehicle	92 (n=6)	978.1 ± 12.5		11.6 ± 0.3	
2	scAAV2.GFP	75 (n=8)	827.0 ± 13.1	2.2	11.7 ± 0.2	0.29 ± 0.5
	Vehicle	75 (n=8)	824.8 ± 14.1		11.6 ± 0.2	

C.

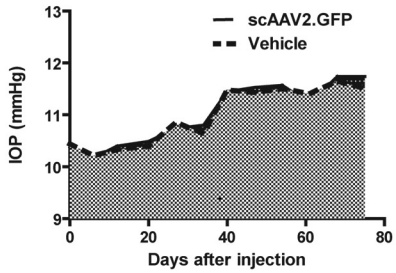

FIGURE 5. Effect of a single IC injection of scAAV2.GFP on the IOP of living rats. The rats were injected with equivalent volumes of scAAV2.GFP (OS; 3–6 × 109 VP) and vehicle (OD). IOPs were measured, before injection ($t \leq 0$ days) and at weekly postinjection intervals, in sedated rats using an induction impact tonometer with a calibrated probe. Results were from two separate, representative experiments ($n = 8$ each) over the course of 92 and 75 days. (**A**) Time course of IOPs with tonometer values converted to mm Hg (mean ± SE). The IOP of the viral-injected eyes at the end of the experiment was not significantly different from baseline and/or from eyes injected with vehicle. (**B**) IOP parameters calculated in scAAV2.GFP- and vehicle-treated eyes. Integral IOPs (cumulative IOP exposure, in mm Hg-days) and peak IOP (maximum IOP elevation during the experiment) were not significantly different between virus- and vehicle-treated eyes. (**C**) Graphic representation of the integral IOP of the average IOPs in experiment 2 in eyes injected with scAAV2.GFP and vehicle. *Dark gray area* between the viral and vehicle control constitutes the IOP–integral difference.

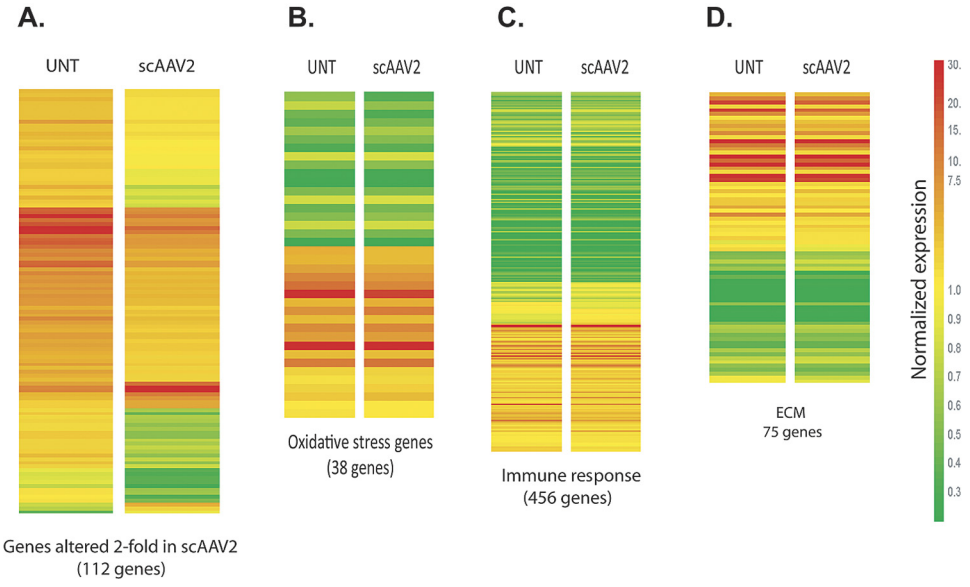

FIGURE 6. Heat maps of sets of genes expressed in HTM cells infected with scAAV2.GFP and untreated control cells. Primary HTM cells were infected with scAAV2.GFP (~1000 VP/cell; scAAV2) and harvested at 7 days after injection. Untreated (UNT) cells grown in parallel were used as a control. RNA was hybridized to microarray chips and analyzed with gene expression software. Expression signals in each chip were compared to a median value. Change from the median is visually represented by a color assignment (scale at *right*). Each row represents the expression of a single gene, and each column contains the genes selected in each category. (**A**) Expression levels of the total number of genes altered more than twofold in scAAV2.GFP-infected cells. (**B**) Expression levels of oxidative stress genes generated from the ontology gene list. (**C**) Expression levels of immune response genes generated from the ontology gene list. (**D**) Expression levels of extracellular matrix (ECM) genes generated from the ontology gene list. Most of the altered genes in scAAV were downregulated from the UNT. Expression of genes in the selected gene lists was barely affected in the scAAV2.GFP-infected cells.

−2.3), chemokine (*C-X-C*) ligand 6 (*CXCL6,* FC −2.6), matrix Gla (*MGP,* FC −3.3), pigment epithelium-derived factor (*PEDF,* FC −2.7), fibulin 1 (*FBLN1,* FC −2.8), osteoglycin (*OGN,* FC −2.7), and secretogranin (*SCG2,* FC −2.5). For validation of the downregulation obtained in the chip, we selected three genes (*MGP*, *OGN*, and *SCG2*), and measured their normalized (18S) differential expression by real-time PCR. Results from triplicate samples showed that the three genes were downregulated on scAAV infection: *MGP* −7.5-fold, *OGN* −19.7-fold, and *SCG2* −5.5-fold. The FCs obtained showed a higher dynamic range than those in the DNA chip, a phenomenon known to occur between quantitative PCR and microarrays.[53]

Examination of the differential expression on the second set of chips, where the HTM cells had received about one tenth the number of VP revealed, concordantly, an even lower difference between scAAV2-infected cells and untreated. The percentage of genes assigned as present and absent between the treated and untreated cells was very similar. The percentage present in the scAAV2-infected cells was 53.9% (12,012/22,277), whereas the untreated was 53.7% (11,962/22,277).

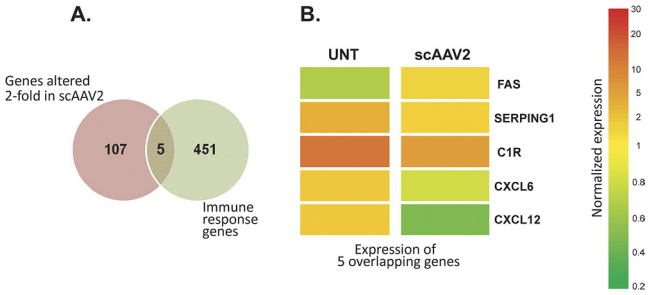

FIGURE 7. Venn diagrams of genes altered more than twofold and immune response genes. Each circle represents one gene list category. Intersections indicate the number of genes that are shared between the two categories. (**A**) Genes shared by the lists of altered twofold and immune response genes. (**B**) Heat map of the five immune response genes which were altered more than twofold. Only one immunorelated gene (FAS) of the 456 was upregulated, whereas the other four were downregulated in scAAV2.GFP-infected cells. This adeno-associated vector had a negligible effect on immune response genes.

The percentage of absent genes was 39.5% (8,793/22,277) for the scAAV2-infected cells and 40.3% (8,972/22,277) for the untreated, respectively. In addition, the subset of genes that were turned on (absent to present) or turned off (present to absent) by infection of the HTM cells with scAAV2.GFP was very small, amounting to 16 genes that were turned on (0.07%) and 10 genes that were turned off (0.04%) in the infected cells. Comparison of expression chips of scAAV2-infected versus untreated cells showed that these lower VP-infected cultures had 17 annotated nonredundant genes (0.08%) with expression that was altered more than twofold. Of these, 6 genes were upregulated and the remaining 11 were downregulated. Three of these genes, *FBLN1*, *OGN*, and *MGP* were downregulated to a lower extent: FC −1.6, −1.9, and −1.1, respectively. Two of the genes, *SFRP1* and *CXCL6*, were upregulated: FC 1.2 and 1.3, respectively.

Altogether these analyses indicate that at the molecular level, scAAV2 has a very minor, if any, deleterious effect on the human trabecular meshwork.

Antibodies to Viral Capsid, Transgene, and Cellular Immune Response

To assess whether there was a systemic humoral immune response to the viral capsid or to the transgene, we determined the levels (as reflected by absorbance at 405 nm) of capsid and GFP antibodies in the serum of the rats and monkeys by ELISA. For the capsid, 1×10^9 scAAV2.GFP VP were bound to 96-well plates overnight, incubated with serial dilutions of rat and monkey sera and followed by incubation with an HRP-conjugated goat anti-rat or -monkey antibody and developed with an HRP substrate. For the positive control, a commercial rabbit anti-AAV2 capsid protein was used as the primary antibody and a HRP-conjugated goat anti-rabbit as a secondary antibody. For the transgene, plates were coated with 0.25 μg (rats) or 0.50 μg (monkeys) of recombinant GFP. Positive control was a commercial rabbit anti-GFP antibody.

After obtaining preinjection serum, the rats were injected intracamerallly with 3 to 6×10^9 VP of scAAV2.GFP as indicated earlier. At 3.5 months after injection, ELISA of pooled serum from rats of the same treatment group showed a mini-

TABLE 2. Systemic Humoral Response after Intracameral Injection of scAAV2

Day	Total Capsid Antibody	Total Transgene GFP Antibody
Rats		
Before injection	0.28 ± 0.02	−0.06 ± 0.00
Day 105	0.40 ± 0.02	−0.04 ± 0.00
Positive control	0.77 ± 0.07	1.75 ± 0.00
Monkeys		
Monkey 1		
Before injection	0.16 ± 0.02	−0.01 ± 0.02
Day 240	0.34 ± 0.05	1.30 ± 0.00
Monkey 2		
Before injection	0.11 ± 0.01	0.13 ± 0.00
Day 240	0.23 ± 0.00	−0.05 ± 0.03
Positive control	0.89 ± 0.01	1.68 ± 0.06

Rat serum dilutions: 1:128 (capsid) and 1:40 (GFP); monkey serum dilutions: 1:80 (capsid) and 1:40 (GFP); positive control dilutions: 1:200 (capsid) and 1:100 (GFP).

mal increase in antibody levels against the viral capsid ($P = 0.05$; Table 2). There was no increased antibody response to transgene GFP, and a significant slight decrease was observed ($P = 0.02$; Table 2). Serum from each of the monkeys was analyzed separately at 8 months after injection. ELISA of serum from monkey 1, in which the transgene expression had disappeared at 70 days after development of a seemingly unrelated inflammation, demonstrated that the scAAV intracameral injection elicited a low, albeit significant, immune response against the viral capsid ($P = 0.03$; Table 2). In this monkey, there was a significant increase in antibody titer against the GFP transgene ($P = 0.000004$). ELISA of serum from monkey 2, in which transgene expression was still noninvasively observed after 2.3 years, resulted in low levels of systemic antibodies against the viral capsid ($P = 0.0004$) and a significant decrease against the transgene GFP ($P = 0.02$).

To determine whether the disappearance of reporter expression (fluorescence) in monkey 1 was due to a cell-mediated immune response against the transgene (GFP), we isolated PBMCs and tested their proliferative response against GFP in a primary proliferation assay. At 11 months after injection, blood was shipped to us overnight at room temperature from the laboratory of one of the authors (PLK), soon after it was obtained. PBMCs (22 hours later) were isolated and cultured in the absence or presence of 10 μg/well of rGFP (no good GFP epitope is known to design an antigenic peptide, and no library of GFP peptides was available), or stimulated with PMA and ionomycin (2 and 50 ng/well, respectively). The cells were incubated for 5 days to allow antigen processing and presentation to T cells. Proliferative response was expressed in counts per minute, which were used to calculate the SI. The results showed that monkey 1, which was "silent," had a significant T-cell proliferative response against the transgene GFP (SI, 3.8), whereas no detectable proliferation was observed in monkey 2 (Fig 8).

DISCUSSION

In this study, we showed for the first time that the self-complementary AAV viral vector overrides the lack of AAV trabecular meshwork transduction, not only in cell and human organ culture[36] but in living animals. A single intracameral injection of the scAAV2 with a CMV-driven GFP in rats and monkeys resulted in very efficient expression of the transgene in the trabecular meshwork. In contrast to the delayed transduction of AAV in the living retina, the expression of the same transgene carried by scAAV in the trabecular meshwork had an early onset, confirming that the rate-limiting step of AAV transduction of this eye tissue was the inability of the virus to convert its ss genome to double stranded.[36] The expression of the transgene in the living animals was long term. In the rat, the last point measured was 3.5 months, and in monkeys, the expression of the transgene, as observed by noninvasive gonioscopy, is ongoing at 2.35 years after a single intracameral injection.

As expected with a gene under the control of a ubiquitous viral promoter, localization of the transgene protein was seen in anterior segment tissues other than the trabecular meshwork by fluorescence and immunohistochemistry. In rats, expression appeared in the corneal endothelium, both faces of the iris, and in the ciliary body. In the monkey, expression was also strong in the ciliary muscle and curiously, very strong in the posterior face of the iris. This iris posterior face tropism was not observed in the rat. Although a needle placement position during the injection could not be excluded, the marked difference observed in the posterior iris in the monkey seems more likely to be due to a different tropism of the virus for the same cell type in the two species. Ongoing experiments in our laboratory in which additional scAAV serotypes were used in the rat indicate that while the trabecular meshwork is transduced efficiently in all pseudotypes tried (2/2, 2/5, and 2/8), different anterior segment patterns of transduction were

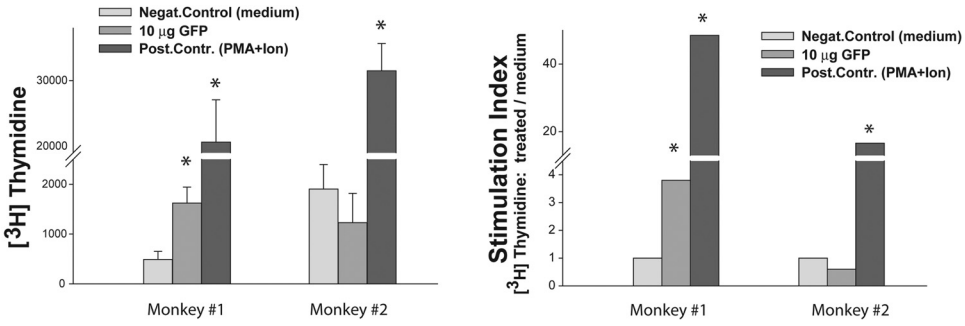

FIGURE 8. PBMC proliferative response against the GFP in monkeys. PBMCs derived from the blood of monkeys 1 and 2 were plated at 2 × 105 cells/well and cultured without antigen or with GFP at 10 μg/well. A stimulation with PMA/ionomycin was used as a positive control. Cells were cultured in triplicate wells for 5 days, and proliferation was assessed by measurement of [3H]-thymidine incorporation. The results are presented as an average counts per minute ± SE or as a stimulation index (SI: cpm in stimulated wells/cpm in unstimulated wells). Statistical analysis was performed by Student's *t*-test. $^*P < 0.05$.

observed with each of the serotypes. These observations highlight the importance of tailoring a particular viral vector for the gene transfer application required.

As when AAV and scAAV vectors transduce the retina of living animals and humans,[54,55] these viruses appear also to be very safe for the trabecular meshwork. Systematic IOP measurements and evaluations showed no differences between the eyes injected with the scAAV2.GFP and their contralateral eyes injected with vehicle. Clinical parameters, including assessment of corneal clarity and inflammation by direct observation and biomicroscopy, revealed a normal-appearing viral-injected eye. In the case of the monkeys, normal behavior (interaction with other monkeys, watching TV) was observed and animals maintained normal visual acuity (able to easily grasp small treats). No humoral or cellular-mediated responses were observed in any of the transgene-expressing animals.

The disappearance of transgene expression of monkey 1 at 70 days after injection followed the development of clinical symptoms suggestive of inflammatory changes in the anterior chamber. The data suggest that the cause of the loss of scAAV2-mediated GFP expression in monkey 1 was due to an immune response to the transgene and not to the scAAV virus. The PMBC cell proliferation assays showed that this monkey had a significant T-cell proliferative response against the GFP, indicating that the disappearance of the GFP expression was probably due to the elimination of GFP-expressing cells by the T lymphocytes. A recent study reported that AAV.GFP injected into the liver in monkeys caused an immune response and loss of expression of the GFP transgene, whereas no response to the viral capsid was observed. This led the investigators to conclude that GFP in monkeys is immunogenic.[56] Since we used the same scAAV2.GFP vector for the two separate monkeys and obtained distinct durations of expression, it is conceivable that the different GFP immune response observed in monkey 1was due to a more efficient GFP antigen presentation by the peripheral blood or local antigen-presenting cells (APCs), leading to the influx of T cells to the trabecular meshwork. The differences in the genetic background between the two animals could have contributed to a different efficiency of antigen presentation, as reflected by different immunogenicity of GFP in two animals.

Finally, comparison arrays between scAAV2-infected and vehicle-treated primary HTM cells showed a minimal effect of the virus on the modulation of the cells' gene expression. The results obtained do not significantly differ from those that have been published by our group and others on the effect of AAV viruses in the cells' transcriptome.[36,57] Only 0.5% of the 22,283 genes of the array were altered more than twofold and of those, most were downregulated. Overall, the altered expression was low to moderate, with only 10 genes upregulated more than twofold and the highest altered gene having a value of less than sixfold (−5.7-fold; Supplementary Table S1, [INSERT URL]). No genes reported to be relevant in the trabecular meshwork[40,41,58] were on the list of twofold upregulated genes. However, the downregulated gene list contained a few genes that have been shown to be altered under known insults to the trabecular meshwork tissue, such as elevated IOP, dexamethasone (DEX), and transforming growth factor-β2 (TGFβ2).[59–61] Thus, SFRP1 is a Wnt pathway antagonist gene which is upregulated in response to elevated IOP[62] and whose overexpression induced high IOP in mice.[10] The cytokine CXCL6 and MGP, an inhibitor of calcification, were found among the genes most altered by high IOP[62]; in addition, MGP was downregulated in glaucomatous tissues and upregulated by TGFβ2.[63] PEDF, a neuroprotector; OGN, a calcification-related protein; and SCG2, a neuropeptide precursor involved in secretion modulation, were upregulated by high IOP[62]; in addition PEDF was specifically induced by DEX,[41,64] OGN was induced by TGFβ2[65] and found in a glaucoma proteomic analysis,[66] and SCG2 was reduced by DEX.[41,67] Downregulation of SCG2 by the AAV2 virus had been observed in the trabecular meshwork cells.[36] FBLN1, a secreted glycoprotein that becomes incorporated into fibrillar ECM on binding to calcium, is also altered by DEX.[41] Only five immune-related genes were found to be present in the list of twofold altered genes, an indication of the low immunogenicity of this vector. Of the five, FAS, a member of the tumor necrosis factor superfamily was upregulated, whereas the two cytokines CXCL6 and CXCL12 were among the most downregulated. Modulation of these genes by scAAV2 infection could have some beneficial or detrimental effect in the trabecular meshwork and should be taken into account when using these vectors.

In summary, the results of this study indicate that the scAAV viral vectors, as well as the original AAV vectors, are very safe for gene therapy in the eye of a living animal. In addition, and in contrast to AAV, the scAAV vectors are able to transduce the trabecular meshwork in vivo. This transduction is long term and has a very rapid onset. The intensity of the GFP expression could be observed at 4 days after injection and lasted at least 3.5 months in rats (assessed by histology) and is ongoing after 2.3 years in a monkey (as observed by noninvasive goniophotography). The scAAV vectors proved to maintain all the safe clinical characteristics of the AAV vectors, which to date are the preferred gene therapy vectors for retinal diseases.[54] Because of the need in glaucoma to develop therapies tailored to restore the function of the trabecular meshwork, the scAAV vectors emerge as strong candidates for the treatment of this disease by gene therapy. Several potentially therapeutic genes have been identified by us and others in recent years.[10,40,41,68,69] This, together with a complete evaluation of different scAAV serotypes (in process), will further contribute to a better targeted transgene delivery and to the goal of modulating the function of the outflow pathway by safe gene transfer to the trabecular meshwork.

Acknowledgments

The authors thank John Danias and Thomas Mittag for providing IOP measurement advice, Chengwen Li and Rachel Caspi for discussions on AAV and eye immunology, John Peterson for expert assistance with goniophotography, and B'Ann Gabelt for assistance with monkey perfusions.

References

1. Streilein JW. *Immune Response and the Eye*. Boston: Karger; 1999.
2. Quigley HA. Number of people with glaucoma worldwide. *Br J Ophthalmol.* 1996;80:389–393.
3. Quigley HA, Vitale S. Models of open-angle glaucoma prevalence and incidence in the United States. *Invest Ophthalmol Vis Sci.* 1997;38:83–91.
4. Budenz DL, Bennett J, Alonso L, Maguire A. In vivo gene transfer into murine corneal endothelial and trabecular meshwork cells. *Invest Ophthalmol Vis Sci.* 1995;36:2211–2215.
5. Millar JC, Pang IH, Wang WH, Wang Y, Clark AF. Effect of immunomodulation with anti-CD40L antibody on adenoviral-mediated transgene expression in mouse anterior segment. *Mol Vis.* 2008; 14:10–19.
6. Kee C, Sohn S, Hwang JM. Stromelysin gene transfer into cultured human trabecular cells and rat trabecular meshwork in vivo. *Invest Ophthalmol Vis Sci.* 2001;42:2856–2860.
7. Borrás T, Gabelt BT, Klintworth GK, Peterson JC, Kaufman PL. Non-invasive observation of repeated adenoviral GFP gene delivery to the anterior segment of the monkey eye in vivo. *J Gene Med.* 2001;3:437–449.
8. Borrás T. Recent developments in ocular gene therapy. *Exp Eye Res.* 2003;76:643–652.

9. Andrawiss M, Maron A, Beltran W, et al. Adenovirus-mediated gene transfer in canine eyes: a preclinical study for gene therapy of human uveal melanoma. *J Gene Med.* 2001;3:228–239.
10. Wang WH, McNatt LG, Pang IH, et al. Increased expression of the WNT antagonist sFRP-1 in glaucoma elevates intraocular pressure. *J Clin Invest.* 2008;118:1056–1064.
11. Hamilton MM, Brough DE, McVey D, Bruder JT, King CR, Wei LL. Repeated administration of adenovector in the eye results in efficient gene delivery. *Invest Ophthalmol Vis Sci.* 2006;47:299–305.
12. Rasmussen H, Chu KW, Campochiaro P, et al. Clinical protocol: an open-label, phase I, single administration, dose-escalation study of ADGVPEDF.11D (ADPEDF) in neovascular age-related macular degeneration (AMD). *Hum Gene Ther.* 2001;12:2029–2032.
13. Borrás T, Porterfield E, Amalfitano A, Vittitow JRL. Adenoviral vector gene transfer to the anterior segment of the brown Norway rats. *Exp Eye Res.* 2002;72(suppl 2):17.
14. Borrás T, Tamm ER, Zigler JS, Jr. Ocular adenovirus gene transfer varies in efficiency and inflammatory response. *Invest Ophthalmol Vis Sci.* 1996;37:1282–1293.
15. Hoffman LM, Maguire AM, Bennett J. Cell-mediated immune response and stability of intraocular transgene expression after adenovirus-mediated delivery. *Invest Ophthalmol Vis Sci.* 1997;38:2224–2233.
16. Brooks AR, Harkins RN, Wang P, Qian HS, Liu P, Rubanyi GM. Transcriptional silencing is associated with extensive methylation of the CMV promoter following adenoviral gene delivery to muscle. *J Gene Med.* 2004;6:395–404.
17. Khare PD, Loewen N, Teo W, et al. Durable, safe, multi-gene lentiviral vector expression in feline trabecular meshwork. *Mol Ther.* 2008;16:97–106.
18. Barraza RA, Rasmussen CA, Loewen N, et al. Prolonged transgene expression with lentiviral vectors in the aqueous humor outflow pathway of nonhuman primates. *Hum Gene Ther.* 2009;20:191–200.
19. Challa P, Luna C, Liton PB, et al. Lentiviral mediated gene delivery to the anterior chamber of rodent eyes. *Mol Vis.* 2005;11:425–430.
20. Cheng L, Sapieha P, Kittlerova P, Hauswirth WW, Di Polo A. TrkB gene transfer protects retinal ganglion cells from axotomy-induced death in vivo. *J Neurosci.* 2002;22:3977–3986.
21. Martin KR, Quigley HA, Zack DJ, et al. Gene therapy with brain-derived neurotrophic factor as a protection: retinal ganglion cells in a rat glaucoma model. *Invest Ophthalmol Vis Sci.* 2003;44:4357–4365.
22. McGee Sanftner LH, Abel H, Hauswirth WW, Flannery JG. Glial cell line derived neurotrophic factor delays photoreceptor degeneration in a transgenic rat model of retinitis pigmentosa. *Mol Ther.* 2001;4:622–629.
23. Acland GM, Aguirre GD, Ray J, et al. Gene therapy restores vision in a canine model of childhood blindness. *Nat Genet.* 2001;28:92–95.
24. Promising results in phase I gene therapy trial for blinding disease [press release]. Bethesda, MD: National Institutes of Health, National Eye Institute; September 23, 2008. Available at: http://www.nei.nih.gov/news/pressreleases/092308.asp. Accessed March 2009.
25. Muzyczka N. Use of adeno-associated virus as a general transduction vector for mammalian cells. *Curr Top Microbiol Immunol.* 1992;158:97–129.
26. Berns KI, Linden RM. The cryptic life style of adeno-associated virus. *Bioessays.* 1995;17:237–245.
27. Grieger JC, Samulski RJ. Adeno-associated virus as a gene therapy vector: vector development, production and clinical applications. *Adv Biochem Eng Biotechnol.* 2005;99:119–145.
28. Choi VW, Asokan A, Haberman RA, Samulski RJ. Production of recombinant adeno-associated viral vectors for in vitro and in vivo use. *Curr Protoc Mol Biol.* 2007;Chapter 16:Unit 16.25.
29. Rivera VM, Gao GP, Grant RL, et al. Long-term pharmacologically regulated expression of erythropoietin in primates following AAV-mediated gene transfer. *Blood.* 2005;105:1424–1430.
30. Zaiss AK, Muruve DA. Immune responses to adeno-associated virus vectors. *Curr Gene Ther.* 2005;5:323–331.
31. Yuasa K, Sakamoto M, Miyagoe-Suzuki Y, et al. Adeno-associated virus vector-mediated gene transfer into dystrophin-deficient skeletal muscles evokes enhanced immune response against the transgene product. *Gene Ther.* 2002;9:1576–1588.
32. Vandenberghe LH, Wilson JM. AAV as an immunogen. *Curr Gene Ther.* 2007;7:325–333.
33. Brockstedt DG, Podsakoff GM, Fong L, Kurtzman G, Mueller-Ruchholtz W, Engleman EG. Induction of immunity to antigens expressed by recombinant adeno-associated virus depends on the route of administration. *Clin Immunol.* 1999;92:67–75.
34. Daya S, Berns KI. Gene therapy using adeno-associated virus vectors. *Clin Microbiol Rev.* 2008;21:583–593.
35. Borrás T, Brandt CR, Nickells R, Ritch R. Gene therapy for glaucoma: treating a multifaceted, chronic disease. *Invest Ophthalmol Vis Sci.* 2002;43:2513–2518.
36. Borrás T, Xue W, Choi VW, et al. Mechanisms of AAV transduction in glaucoma-associated human trabecular meshwork cells. *J Gene Med.* 2006;8:589–602.
37. McCarty DM, Fu H, Monahan PE, Toulson CE, Naik P, Samulski RJ. Adeno-associated virus terminal repeat (TR) mutant generates self-complementary vectors to overcome the rate-limiting step to transduction in vivo. *Gene Ther.* 2003;10:2112–2118.
38. McCarty DM, Monahan PE, Samulski RJ. Self-complementary recombinant adeno-associated virus (scAAV) vectors promote efficient transduction independently of DNA synthesis. *Gene Ther.* 2001;8:1248–1254.
39. Ferrari FK, Samulski T, Shenk T, Samulski RJ. Second-strand synthesis is a rate-limiting step for efficient transduction by recombinant adeno-associated virus vectors. *J Virol.* 1996;70:3227–3234.
40. Borrás T. Mechanosensitive genes in the trabecular meshwork at homeostasis: elevated intraocular pressure and stretch. In: Tombran-Tink J, Barnstable CJ, Shields MB, eds. *Mechanisms of the Glaucomas: Disease Processes and Therapeutic Modalities*. New York: Humana Press, Inc.; 2008:329–362.
41. Borrás T. What is functional genomics teaching us about intraocular pressure regulation and glaucoma. In: Civan MM, ed. *The Eye's Aqueous Humor.* 2nd ed. San Diego: Elsevier, Inc.; 2008:193–229.
42. Xiao X, Li J, Samulski RJ. Production of high-titer recombinant adeno-associated virus vectors in the absence of helper adenovirus. *J Virol.* 1998;72:2224–2232.
43. Zolotukhin S, Byrne BJ, Mason E, et al. Recombinant adeno-associated virus purification using novel methods improves infectious titer and yield. *Gene Ther.* 1999;6:973–985.
44. Shi W, Bartlett JS. RGD inclusion in VP3 provides adeno-associated virus type 2 (AAV2)-based vectors with a heparan sulfate-independent cell entry mechanism. *Mol Ther.* 2003;7:515–525.
45. Borrás T, Rowlette LL, Erzurum SC, Epstein DL. Adenoviral reporter gene transfer to the human trabecular meshwork does not alter aqueous humor outflow: relevance for potential gene therapy of glaucoma. *Gene Ther.* 1999;6:515–524.
46. McCown TJ. Adeno-associated virus-mediated expression and constitutive secretion of galanin suppresses limbic seizure activity in vivo. *Mol Ther.* 2006;14:63–68.
47. Danias J, Kontiola AI, Filippopoulos T, Mittag T. Method for the noninvasive measurement of intraocular pressure in mice. *Invest Ophthalmol Vis Sci.* 2003;44:1138–1141.
48. Kontiola AI, Goldblum D, Mittag T, Danias J. The induction/impact tonometer: a new instrument to measure intraocular pressure in the rat. *Exp Eye Res.* 2001;73:781–785.
49. Kaufman PL, Davis GE. "Minified" Goldmann applanating prism for tonometry in monkeys and humans. *Arch Ophthalmol.* 1980;98:542–546.
50. Zhang X, Tang Y, Sujkowska D, et al. Degenerate TCR recognition and dual DR2 restriction of autoreactive T cells: implications for the initiation of the autoimmune response in multiple sclerosis. *Eur J Immunol.* 2008;38:1297–1309.
51. Xiao W, Warrington KH Jr, Hearing P, Hughes J, Muzyczka N. Adenovirus-facilitated nuclear translocation of adeno-associated virus type 2. *J Virol.* 2002;76:11505–11517.
52. Hu Y, Gabelt BT, Kaufman PL. Monkey organ-cultured anterior segments: technique and response to H-7. *Exp Eye Res.* 2006;82:1100–1108.
53. Carmel JB, Galante A, Soteropoulos P, et al. Gene expression profiling of acute spinal cord injury reveals spreading inflammatory signals and neuron loss. *Physiol Genomics.* 2001;7:201–213.

54. Maguire AM, Simonelli F, Pierce EA, et al. Safety and efficacy of gene transfer for Leber's congenital amaurosis. *N Engl J Med.* 2008;358:2240–2248.
55. Natkunarajah M, Trittibach P, McIntosh J, et al. Assessment of ocular transduction using single-stranded and self-complementary recombinant adeno-associated virus serotype 2/8. *Gene Ther.* 2008;15:463–467.
56. Gao G-P, Calcedo R, Wang L, et al. Transgene immunity dictates the stability of efficient EGFP gene transfer by conventional (ss) and self complementary (sc) AAV7 vectors in nonhuman primate liver. ASGT (American Society of Gene Therapy) 2007:Abstract 1086.
57. Stilwell JL, Samulski RJ. Role of viral vectors and virion shells in cellular gene expression. *Mol Ther.* 2004;9:337–346.
58. Borrás T. Gene expression in the trabecular meshwork and the influence of intraocular pressure. *Prog Retin Eye Res.* 2003;22:435–463.
59. Gordon MO, Beiser JA, Brandt JD, et al. The Ocular Hypertension Treatment Study: baseline factors that predict the onset of primary open-angle glaucoma. *Arch Ophthalmol.* 2002;120:714–720.
60. Armaldy MF, Becker B. Intraocular pressure response to topical corticosteroids. *Fed Proc.* 1965;24:1274–1278.
61. Lütjen-Drecoll E. Morphological changes in glaucomatous eyes and the role of TGFbeta2 for the pathogenesis of the disease. *Exp Eye Res.* 2005;81:1–4.
62. Comes N, Borrás T. Individual molecular response to elevated intraocular pressure in perfused postmortem human eyes. *Physiol Genomics.* 2009;38:205–225.
63. Xue W, Comes N, Borrás T. Presence of an established calcification marker in trabecular meshwork tissue of glaucoma donors. *Invest Ophthalmol Vis Sci.* 2007;48:3184–3194.
64. Perruccio EM, Rowlette LL, Comes N, et al. Dexamethasone increases pigment epithelium-derived factor in perfused human eyes. *Curr Eye Res.* 2008;33:507–515.
65. Zhao X, Ramsey KE, Stephan DA, Russell P. Gene and protein expression changes in human trabecular meshwork cells treated with transforming growth factor-beta. *Invest Ophthalmol Vis Sci.* 2004;45:4023–4034.
66. Bhattacharya SK, Rockwood EJ, Smith SD, et al. Proteomics reveal Cochlin deposits associated with glaucomatous trabecular meshwork. *J Biol Chem.* 2005;280:6080–6084.
67. Rozsa FW, Reed DM, Scott KM, et al. Gene expression profile of human trabecular meshwork cells in response to long-term dexamethasone exposure. *Mol Vis.* 2006;12:125–141.
68. Vittitow JL, Garg R, Rowlette LL, Epstein DL, O'Brien ET, Borrás T. Gene transfer of dominant-negative RhoA increases outflow facility in perfused human anterior segment cultures. *Mol Vis.* 2002;8:32–44.
69. Liu X, Hu Y, Filla MS, et al. The effect of C3 transgene expression on actin and cellular adhesions in cultured human trabecular meshwork cells and on outflow facility in organ cultured monkey eyes. *Mol Vis.* 2005;11:1112–1121.